ELSEVIER

www.elsevier.nl/locate/jorganchem

Journal of Organometallic Chemistry 621 (2001) 254–260

Journal of Organometallic Chemistry

Self-assembly of $[Cu(CN)_4]^{3-}$ ions with cationic $\{Me_3Sn\}^+$ or $\{Me_2Sn(CH_2)_3SnMe_2\}^{2+}$ fragments in the presence of a $^nBu_4N^+$ template

Eyck-Michael Poll [a], Jens-Udo Schütze [a], R. Dieter Fischer [a,*], Nicola A. Davies [b], David C. Apperley [b], Robin K. Harris [b]

[a] *Institut für Anorganische und Angewandte Chemie, Universität Hamburg, Martin-Luther-King-Platz 6, 20146 Hamburg, Germany*
[b] *Department of Chemistry, University of Durham, South Road, Durham DH1 3LE, UK*

Received 31 August 2000

Dedicated to Professor H. Brunner on the occasion of his 65th birthday

Abstract

As described earlier, solutions of $^nBu_4NCl$ and $K_3[Cu(CN)_4]$ react with Et_3SnCl to zeolite-like $[(Bu_4N)(Et_3Sn)_2Cu(CN)_4]$ (**1**), but with Me_3SnCl exclusively to $[(Bu_4N)(Me_3Sn)Cu_2(CN)_4]$ (**2**), the crystal structure of which is reported here for the first time. The $^nBu_4N^+$ guest ions of **2** are accommodated between planar, negatively charged layers, wherein three-coordinated Cu(I) ions are interlinked by CN– and $CN{\cdot}SnMe_3{\cdot}NC$ bridges (2:1). The slightly modified new homologue of **2**: $[(^nBu_4N)\{Me_2Sn(CH_2)_3SnMe_2\}_{0.5}Cu_2(CN)_4]$ (**3**), displays an almost identical powder X-ray diffractogram as **2** and, moreover, surprisingly similar solid-state NMR spectra for the nuclei ^{13}C, ^{15}N and ^{119}Sn. A three-dimensional host framework is postulated to encapsulate the $^nBu_4N^+$ guest of **3**, the Sn atoms of adjacent layers being therein tied pair-wise together by trimethylene tethers, $(CH_2)_3$. For further comparison, the solid-state NMR data of the new coordination polymer $[\{Me_2Sn(CH_2)_3SnMe_2\}_{0.5}Au(CN)_2]$ (**5**) are also presented. © 2001 Elsevier Science B.V. All rights reserved.

Keywords: $^nBu_4N^+$ template; Self assembly; Trimethylene tethers; Organotin(IV); Copper (I) cyanide

1. Introduction

Super-Prussian blue [1] derivatives of the organometallic family $[(R_3E)_3M^{III}(CN)_6] \triangleq {}^3_\infty[M^{III}\mu\text{-}\{CNE(R_3)NC\}_3]$ with R = alkyl, E = Sn or Pb and M = Fe, Co, Rh or Ir [2] still resemble the familiar Prussian blue representatives ${}^3_\infty[M\mu\text{-}(CN)_3]$ (usually with $M = 0.5\ M' + 0.5\ M''$) [3] structurally, although their intra-chain M···M separations are about twice as large (i.e. of ca. one nm) as in classical Prussian blue systems. Replacement of the octahedral $M(CN)_6$ by tetrahedral $M(CN)_4$ building blocks would lead to coordination polymers more closely related to zeolites. While numerous zeolite-like polymeric metal cyanides involving the 'classical' M–CN–M′ bridge, and usually a guest cation, G^+, are known, [4,5] the coordination polymer $[(^nBu_4N)(Et_3Sn)_2Cu(CN)_4]$ (**1**), is still unique in displaying the expanded $M{-}CN{-}SnR_3{-}NC{-}M$ bridge [6]. In spite of extensive attempts to prepare, and characterize, further examples of the general type $[G(R_3E)_2Cu(CN)_4]$, only too reluctantly crystallizing products either of the desired composition or of a quite unexpected new type, $[G(R_3E)Cu_2(CN)_4]$, have so far been described [6,7]. Single crystals suitable to determine the crystal structure of the longest known [6] representative of this latter class, $[(^nBu_4N)(Me_3Sn)Cu_2(CN)_4]$ (**2**), could be obtained only most recently. In the present contribution, the supramolecular architecture of **2** will be presented and correlated with extended multinuclear solid-state NMR results. The slightly modified, new product $[(^nBu_4N)\{Me_2Sn(CH_2)_3Sn$-

---

* Corresponding author. Tel.: +49-40-428383100/428383101; fax: +49-40-428382882.

E-mail address: fischer@chemie.uni-hamburg.de (R.D. Fischer).

PII: S0022-328X(00)00747-6

$Me_2\}_{0.5}Cu_2(CN)_4]$ (**3**), which differs from **2** formally in that two methyl groups of each pair of Me_3Sn units are replaced by one $–(CH_2)_3–$ spacer, is also characterized both by its solid-state NMR spectra and its powder X-ray diffractogram (XRD). In view of convincing experimental evidence in favor of a practically isostructural architecture of **2** and **3**, a plausible proposal for the location of the trimethylene tether in the structure of **3** is likewise possible.

2. Preparation of 2 and 3

Both $[(^nBu_4N)(Me_3Sn)Cu_2(CN)_4]$ (**2**) [6] and $[(^nBu_4N)\{Me_2Sn(CH_2)_3SnMe_2\}_{0.5}Cu_2(CN)_4]$ (**3**) were obtained first (as so-called derailment products) when the synthesis of potential zeolite-like homologues of **1** containing tin-bonded alkyl ligands of lower space demand than required by ethyl groups was attempted:

$$\begin{gathered}2Me_3SnCl \text{ (or } ClMe_2Sn(CH_2)_3SnMe_2Cl) \\ + K_3[Cu(CN)_4] + {}^nBu_4NCl \rightarrow 3KCl + \\ [(^nBu_4N)(Me_2SnR)_2Cu(CN)_4] \text{ (R = Me or } (CH_2)_{3/2})\end{gathered} \quad (1)$$

However, according to the C/H/N and metal analyses, which reflected constantly a Sn:Cu ratio of 1:2, exclusively **2** and **3**, respectively, were obtained. Application of the Sn- and Cu-containing reactants in the appropriate stoichiometric ratio afforded **2** and **3**, respectively, in yields of $\geq 85\%$. The optimal route to arrive at **2** or **3** involves two separate steps (Eq. (2)):

$$\begin{gathered}(^nBu_4N)CN + CuCN \\ \rightarrow (^nBu_4N)[Cu(CN)_2];\ R_3SnX + 2(^nBu_4N)[Cu(CN)_2] \\ \rightarrow [(^nBu_4N)(R_3Sn)Cu_2(CN)_4]\downarrow + (^nBu_4N)X \text{ (X = Cl or} \\ \text{Br; R = either exclusively Me,} \\ \text{or Me (2x) and } (CH_2)_{3/2})\end{gathered} \quad (2)$$

Both **2** and **3** are air stable, white solids that decompose above ca. 260 [6] and 170°C, respectively. Single crystals of **2** separated from the mother liquor obtained after precipitation and filtration when it was kept at a temperature of ca. 20°C for several days. Unexpectedly, the elemental analysis of the bulk precipitate resulting for this particular experiment deviated considerably from the data expected for **2**, while both the analytical and spectroscopic results for the crystalline material agreed well with those reported earlier [6]. It might be recalled here that during corresponding, earlier attempts to arrive at suitable crystals of **2** and **3**, single crystals of the likewise, new, completely tin-free host/guest system $[(^nBu_4N)Cu_2(CN)_3]$ (**4**), could occasionally be isolated [8]. The negatively charged host framework $[Cu_2(CN_3)^-]$ of **4** is three-dimensional (3-D), and does not match with the sheet-like 2-D frameworks of other $[(G)Cu_2(CN)_3]$ systems [9,10].

3. Crystal structure of 2

For the negatively charged $[(Me_3Sn)Cu_2(CN)_4^-]$ host framework of **2**, three different structural motifs might in principle be envisaged. One of them could involve just one tetracoordinate Cu(I) center which might build up, in combination with the two potential, rod-like tethers $\{CNCuNC\}^-$ and $\{CNSnMe_3NC\}^-$, either a quasi-diamondoid framework (3-D) or puckered layers (2-D) of the composition $[Cu\{\mu\text{-}CNCuNC\}\{\mu\text{-}CNSn(Me_3)NC\}]$. The second motif could involve no longer unusual [11] $\{Cu_2(\mu_3\text{-}CN)_2\}$ fragments, which might be tied together to infinite frameworks both by CN^- (Cu–CN–Cu) and $\{SnMe_3\}^+$ spacers (CN–Sn–NC). The third motif would make use of CN^- and $CNSnMe_3NC^-$ bridges too (in the ratio 2:1), but exclusively between three-coordinate Cu(I) ions.

The crystal structure analysis has revealed unambiguously the formation of almost planar, infinite layers involving trigonal $\{Cu(CN)_2(NC)\}$ building blocks. Correspondingly, the derailment reaction from Eq. (1) was accompanied by a partial cleavage of the initially chosen $[Cu(CN)_4]^{3-}$ anion. Fig. 1 presents a perspective of the supramolecular structure of **2** along *b*. Owing to eclipsed stacking with an interlayer (Cu···Cu) distance of 7.0819(6) Å, straight hexagonal channels extend along *b*. Selected crystal data and refinement parameters are given in Table 1, and the asymmetric unit of **2** is shown in Fig. 2. As nitrogen and carbon atoms of the Cu–CN–Cu′ bridges cannot be distinguished, their designation as C or N in Fig. 2 must be considered as arbitrary. In striking contrast to the experience with zeolite-derived host/guest systems, where the guest atoms generally tend to be more readily disordered than atoms of the host framework, the $^nBu_4N^+$ ions of **2** are not disordered, while, on the other hand, positions of atoms of the framework component Me_3Sn display notable irregularities. This feature had caused, at a first glance, some irritation in view of the quality of the single crystal studied. Optimal refinement was achieved when each tin atom was assumed to be disordered, adopting four slightly different positions (weight factors: 45, 45, 5, 5%). The methyl groups appear to surround each tin atom almost like a wreath. For their visualization in Fig. 2, only six positions reflecting highest electron density around Sn2 were, somewhat arbitrarily, picked out. Selected interatomic distances and bond angles of **2** are listed in Table 2.

While the fragments Cu–CN–Cu′ and C1–N1–Sn turn out to be almost linear, the N1–Sn–N1′ angle deviates more strongly from 180° than in all earlier reported coordination polymers with M–CN–SnR_3–NC–M bridges (e.g. N–Sn–N′ in **1** [6]: 178.4 ± 0.4°). This unusual nonlinearity has presumably the same, still unclear origin, which is also responsible for the disorder of the Me_3Sn units. Most of the interatomic distances listed in Table 2 match satisfactorily with corresponding literature data (e.g. N–Sn in **1**: 2.33 and 2.34 Å). The situation is notably different for the Sn–C distances (not included in Table 2). If the six positions of major relevance for the Sn–bonded methyl carbon atoms are tentatively divided into two groups, assuming that for each group the three corresponding C–Sn–C′ angles would sum up to 360°, the d(Sn–C) values would range between 2.03 and 2.30 Å. Usually, however, the individual Sn–C bond length in Me_3Sn groups carrying two axial NC ligands varies only between 2.07 and 2.17 Å, although the sum of the three C–Sn–C′ angles may differ notably from 360° [12].

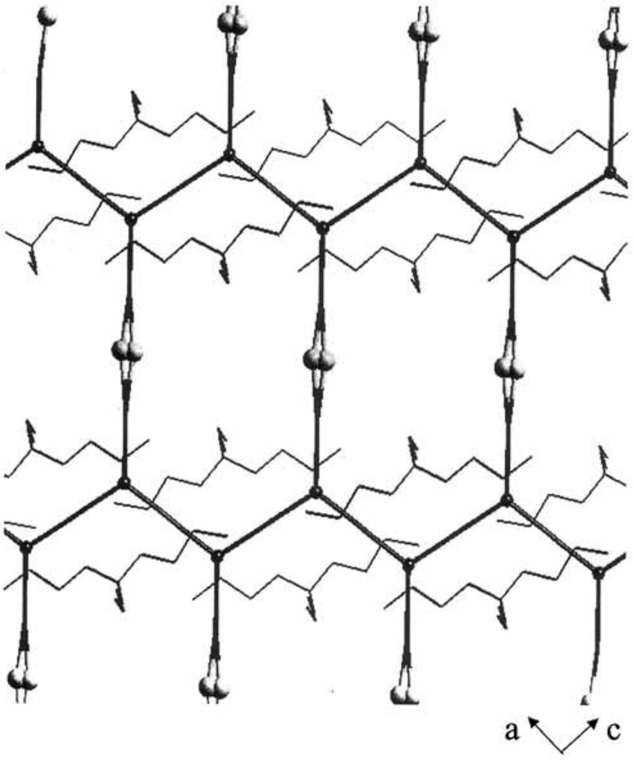

Fig. 1. Perspective of the structure of **2** along *b*. Large spheres: Sn (disordered; major positions only), smaller spheres: Cu; tin-bonded methyl groups have been omitted.

Table 1
Crystal data and structure refinement parameters for [^{n}Bu$_4$N)-(Me_3Sn)$Cu_2(CN)_4$] (**2**)

Empirical formula	$C_{23}H_{45}Cu_2N_5Sn$
Formula weight (g mol^{-1})	637.41
Temperature (K)	173(2)
Wavelength (Å)	0.71073
Crystal system	Monoclinic
Space group	*C*2/*m*
Unit cell dimensions	
a (Å)	16.7353(2)
b (Å)	14.0191(2)
c (Å)	14.08230(10)
α (°)	90
β (°)	106.4950(10)
γ (°)	90
V (Å^3)	3167.93(6)
Z	4
D_{calc} (Mg m^{-3})	1.336
Absorption coefficient (mm^{-1})	2.129
F(000)	1304
Theta range for data collection (°)	1.51–28.97
Index ranges	$-15<h<22$, $-18<k<17$, $-17<l<18$
Reflections collected	10 729
Unique reflections	4109 [$R_{int} = 0.0385$]
Completeness to 2Θ	28.97° 47.0%
Refinement method	Full-matrix least-squares on F^2
Data/restraints/parameters	4109/0/178
Goodness-of-fit on F^2	0.970
Final *R* indices [$I>2\sigma(I)$]	$R_1 = 0.0431$, $wR_2 = 0.1124$
R indices (all data)	$R_1 = 0.0668$, $wR_2 = 0.1267$
Largest difference peak and hole	0.603 and −0.833 e Å^{-3}

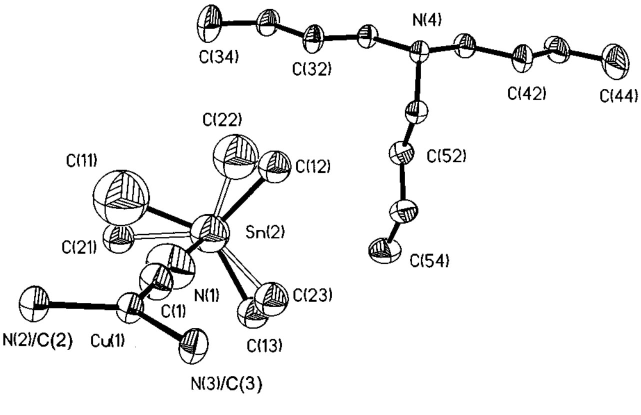

Fig. 2. Asymmetric unit (50% occupation) of **2**, ignoring here the disorder of the Sn atom. C(2) and N(2) have to be considered as fictive labels.

Another unexpected feature accompanying the structural irregularities mentioned above is that the interlayer Sn···Sn separation alternates periodically between 6.1939(12) and 7.8471(12) Å (see Fig. 3). On the other hand, the corresponding Cu···Cu separation varies comparatively little. Interestingly, no other intra- or interlayer Sn···Sn distance in the range of 6.2 ± 0.5 Å is found in the structure of **2**. On the assumption that compound **3** would be virtually isostructural with **2** (vide infra), apart from the requirement that the Sn atoms of **3** must be tied pair-wise together by means of their trimethylene tether, the interlayer Sn···Sn separations indicated in Fig. 3 by straight grey lines would appear to be predestinated to accommodate the (CH$_2$)$_3$ tether. Actually, various crystallographic studies of compounds involving a {Sn(CH$_2$)$_3$Sn} fragment [13] have shown that here the Sn···Sn distance quite consistently adopts values within the range: 6.10–6.35 Å. The ^{n}butyl groups of each ^{n}Bu$_4$N$^+$ ion extend pair-wise parallel and perpendicular to the host layers, respectively, the latter pair remaining ‘crystallographically degenerate’. All bond distances and angles found for the ^{n}Bu$_4$N$^+$ ion except the rather large N–Cα–Cβ angles (Table 2) agree well with corresponding data from the literature [6,8,14].

Table 2
Selected interatomic distances (Å) and bond angles (°) of **2**

Bond distances			
Sn–N1	2.311(4)	C1–N1	1.144(5)
Cu–C1	1.906(3)	C2–N2	1.165(5)
Cu–N2	1.936(3)	C3–N3	1.175(5)
Cu–N3	1.947(2)		
Bond angles			
N4–C31–C32	116.5(3)	C1–N1–Sn	171.9(4)
N4–C41–C42	117.7(3)	N1–Sn–N1′	166.71(19)
N4–C51–C52	115.7(2)	C1–Cu–N2	123.06(14)
C1–Cu–N3	124.10(14)	Cu–N2–C2	172.96(9)
N3–Cu–N2	112.82(10)	Cu–N3–C3	177.1(3)
Cu–C1–N1	179.0(4)		

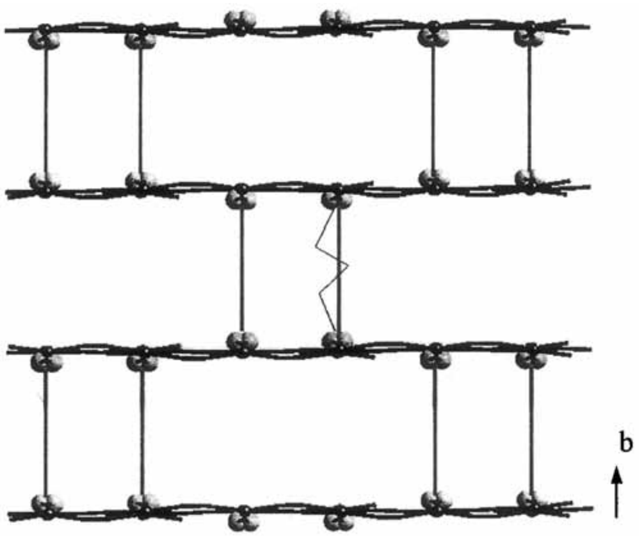

Fig. 3. Perspective of the structure of **2** along the *a*/*c*-diagonal. Tin-bonded methyl groups have been omitted, while the disorder of the tin atoms has been accounted for. Vertical grey lines indicate the shorter Sn···Sn separations suitable to accommodate a (CH$_2$)$_3$ tether (see also the zigzag line in the middle of the figure). The ^{n}Bu$_4$N$^+$ guest ions have also been omitted.

Table 3
Survey of C···N separations (<4.0 Å) between ^{n}Bu$_4$N$^+$ carbon and CN nitrogen atoms of **2**

N atom	C atom	d(C···N) (Å)
N2	C52	3.576(4)
		3.593(4)
	C31	3.814(3)
	C44	3.971(4)
N3	C43	3.568(3)
		3.850(3)
	C52	3.797(4)
		3.862(4)
	C42	3.800(3)
	C41	3.988(3)

The excellent localization of all non-hydrogen atoms of the ^{n}Bu$_4$N$^+$ guest ion also justifies a brief screening in view of C(guest)···N(host) separations short enough to suggest weak, but non-negligible, C–H···N hydrogen bonds (Table 3). Focusing here on C···N distances ≤ 4.0 Å, three comparatively short ones (i.e. of < 3.60 Å) are found, which involve only atoms of the Cu–CN–Cu′ bridges. Cyanide N atoms already coordinated to a metal center are, according to earlier studies [8,12b], less susceptible to interact with potentially bridging hydrogen atoms than terminal cyanide N atoms, which reluctance is clearly reflected by notably more elongated C···N distances. There are, moreover, two comparatively short C···Cu separations of 3.5847(14) and 3.659(2) Å (involving C33 and C44, respectively, and suggesting weak C–H···Cu interactions), which turn out to be even shorter than those found in **4** [8].

4. Powder X-ray diffractometry of 2 and 3

In Fig. 4, the experimental powder X-ray diffractograms (XRD’s) of **2** and **3** are compared with the simulated XRD of **2**, the latter being based on data resulting from the structure analysis of a single crystal (vide supra). All three XRD’s look very similar, suggesting immediately that the finely powdered bulk samples of both **2** and **3** should at least be structurally closely related to crystalline **2**. It should be noted here that usually the lighter atoms of a sample containing heavier metal atoms (i.e. also C, N, O etc.) do not contribute specifically to the diffraction pattern. For instance, it can easily be demonstrated [15] that the simulated XRD’s of the two homologous coordination polymers [(R$_2$Sn)$_3${Co(CN)$_6$}$_2$] with R = ^{n}propyl and ^{n}butyl [16] are almost coincident. The satisfactory agreement of the experimental with the simulated XRD of **2** confirms, moreover, the superiority of the space group *C*2/*m* over e.g. *P*2$_1$/*c*. After corresponding structure refinement and simulation of the XRD for the space group *P*2$_1$/*c*, notably less agreement with the experimental XRD was achieved. Another favorable consequence of the results manifested by Fig. 4 is that the solid-state NMR spectra of **2**, and possibly of **3**, may be interpreted in terms of the asymmetric unit of **2** (see Fig. 2).

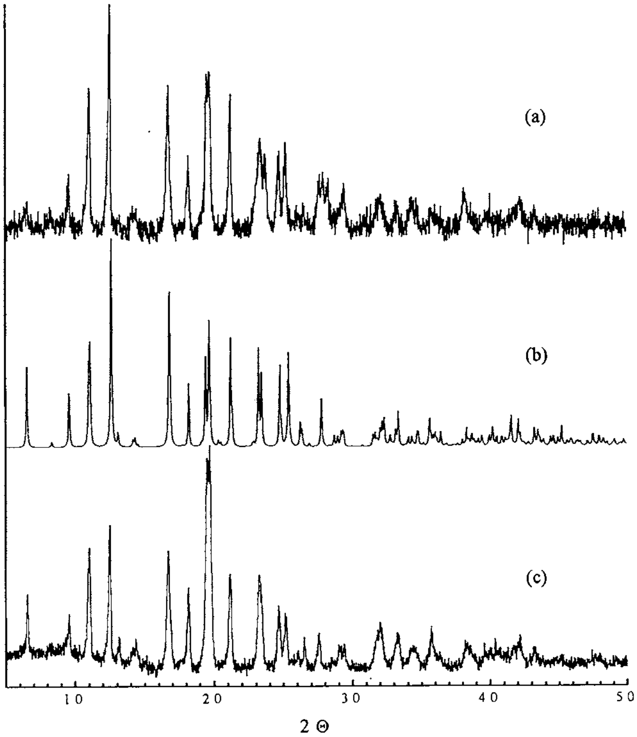

Fig. 4. Comparison of the simulated powder X-ray diffractogram (XRD) of **2** (b) with the experimental XRD's of **2** (a) and **3** (c).

Table 4
Comparison of solid-state NMR data (chemical shifts) of **2**, **3** and **5**

Nucleus	Assignment	Sample		
		2	**3**	**5**
^{119}Sn		−166.0 [a]	−167.8	−87.7
^{15}N	^{n}Bu$_4$N$^+$	−307.7	−307.7	
	CN	−138.1	−138.3	−137.9
^{13}C	MeSn	0.72 [a,b]	0.51 [c]	−2.7, 4.9
	CH$_2$Sn, –CH$_2$–		22.8	23.6
	CN	157, 151, 139 [a]	152	151
	α-CH$_2$ (^{n}Bu)	60.0, 58.3 [a]	60.2, 58.0	
	β-CH$_2$ (^{n}Bu)	24.5 [a]	25.0	
	γ-CH$_2$ (^{n}Bu)	21.8, 20.2 [d], 19.8 [a,d]	21.6, 19.9 [d]	
	δ-CH$_3$ (^{n}Bu)	15.55, 14.51, 13.43 [a]	15.64, 14.39, 13.90	

[a] Data taken from Ref. [6].
[b] $J|\mathrm{SnC}| = 600$ Hz.
[c] $J|\mathrm{SnC}| = 570$ Hz.
[d] Shoulder.

5. CPMAS solid-state magnetic resonance spectra of 2 and 3

The chemical shifts of all resonances of the nuclei ^{13}C, ^{15}N and ^{119}Sn are, as far as detectable in the solid-state NMR spectra of **2** and **3**, listed for comparison in Table 4. Both **2** and **3** give rise to only one ^{119}Sn center band, in spite of the notable disorder of the tin atoms as reflected by the single-crystal X-ray study of **2**. Correspondingly, just one singlet is found for the tin-bonded methyl carbon atoms of **2**, most probably owing to rapid rotation of the Me$_3$Sn group about its N–Sn–N axis [17]. From the manifold of ^{119}Sn spinning side bands of **3**, axial symmetry can be deduced. The corresponding values for **3** are −379 and 0.02 ppm. In each case the asymmetry is within experimental error of zero, i.e. there is essentially axial local electronic symmetry. Only one sharp line is found in the low-frequency range of the ^{15}N spectrum (^{n}Bu$_4$N$^+$ resonance), of both **2** and **3** in accordance with the asymmetric unit for **2**. The cyanide ligands give rise to likewise one, notably broader ^{15}N resonance for the two compounds, although at least two lines would be expected since both N–Cu and N–Sn nitrogens are present. However, while for **2** three cyanide ^{13}C resonances are reported [6], **3** turns out to show just one broad center band. Again, at least two different cyanide carbon atoms are expected according to the asymmetric unit of **2**, although it may be noted that all cyanide carbon atoms are bonded to Cu.

The ^{13}C resonance patterns of all aliphatic carbon atoms present in **2** [6] and **3** look surprisingly similar (Fig. 5). The only extra signal occurring in the spectrum of **3** (at 22.8 ppm) may, in good agreement with earlier findings [18], be attributed to carbon atoms of the (CH$_2$)$_3$ tether. The two tin-bonded methyl groups of **3** give rise to just *one* singlet, suggesting for them equal environments. This feature strongly favors the proposal (vide supra) according to which the (CH$_2$)$_3$ tethers would tie together distinct tin atoms of adjacent framework layers (see also Fig. 3).

The ^{n}butyl groups of the ^{n}Bu$_4$N$^+$ guest ions of **3** give rise, at least for the α-CH$_2$ and δ-CH$_3$ fragments, to

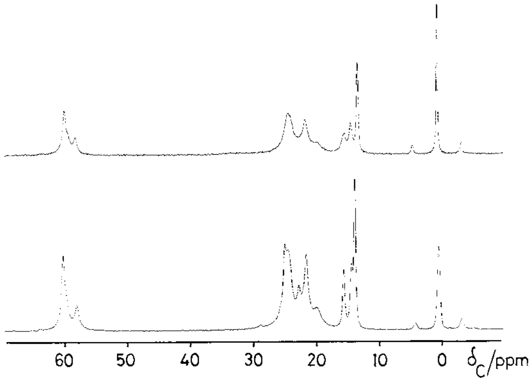

Fig. 5. Carbon-13 CPMAS spectra of **2** (top) and **3** (bottom). Both were recorded with a 1 s recycle delay. For **2**, the spectrum was obtained from 1000 repetitions with a contact time of 5 ms and a spin rate of 4.75 kHz. For **3**, the spectrum was obtained from 7100 repetitions with a 10 ms contact time and a spin rate of 4.80 kHz. The spectra are plotted without any artificial linebroadening.

two signals with an approximate intensity ratio of 1:3 (the more intense signal of the CH_3 groups including also a close-lying shoulder). This intensity ratio may tentatively be correlated with the asymmetric unit of **2** according to which three crystallographically nonequivalent butyl groups are present in the lattice. Accounting also for the shoulder, apparently all three different δ-CH_3 groups (one of which counting twice) can actually be distinguished. While also the γ-CH_2 groups seem to give rise to two separate signals of different intensities, the β-CH_2 groups generate one faintly split signal only.

For further comparison, the solid-state NMR data of the new, $^{n}Bu_4N^+$-free coordination polymer $[\{Me_2Sn(CH_2)_3SnMe_2\}_{0.5}Au(CN)_2]$ (**5**) are also included in Table 4. As expected, the ^{119}Sn shift of **5** differs strongly from the shifts of the two negatively charged frameworks of **2** and **3**, but resembles the earlier reported [19] δ value of $[Et_3SnAu(CN)_2]$ (− 64 ppm). The two ^{13}C shift values of **5** listed in the MeSn entry might refer either to two crystallographically nonequivalent methyl groups or to just one methyl carbon and one (likewise tin-bonded) methylene carbon atom. However, the strong ^{13}C signal at 23.6 ppm suggests the tether CH_2 carbons to resonate there. The ethyl carbon resonances of $[Et_3SnCu(CN)_2]$ were found at 11.0 and 11.7 ppm [19]. The cyanide ^{13}C and ^{15}N shifts of **5** do not differ from those of **2** and **3**.

6. Conclusions

Although the quality of the crystal structure analysis of **2** might be somewhat affected by the significant disorder of the tin and carbon atoms of the Me_3Sn unit, any severe doubts in the supramolecular architecture based on that stucture analysis can be rejected in accounting also for the detailed solid-state NMR studies of **2** and **3**. Owing to almost identical powder X-ray diffractograms (Fig. 4), both compounds are practically isostructural and display, consequently, for the nuclei ^{13}C, ^{15}N and ^{119}Sn surprisingly similar NMR spectra (Table 4). The observed number of resonances to be ascribed to nuclei of distinct molecular fragments never exceeds the corresponding number predicted by the (crystallographically deduced) asymmetric unit, if the aforementioned disorder is fully ignored. The latter feature casts some doubt in the appearance of equally pronounced disorder in all of the samples. Whenever the observed number of resonances turns out to be lower than expected, reasonable explanations can be found (e.g. rapid Me_3Sn rotation).

It may be worth recalling that the crystal structure of **2** is optimal in offering a suitable location for the $(CH_2)_3$ tether (of **3**): Not only two tin atoms with the required Sn···Sn separation (vide supra) are available, each of which would carry (in **3**) two equivalent methyl groups (as confirmed by the ^{13}C-NMR spectrum of **3**). Moreover, the $(CH_2)_3$ tether can be accommodated in interlayer voids spatially well separated from the ^{n}butyl groups of the $^{n}Bu_4N^+$ guest ion (see Fig. 3). The latter feature is clearly confirmed by the surprising similarity of all ^{13}C resonances of the ^{n}butyl carbon atoms in the spectra of **2** and **3.**

Finally, the appearance of two Raman and one infrared active ν(CN) bands in the vibrational spectra of **3** (Ra: 2128 and 2115 cm^{-1}; IR: 2111 cm^{-1}) may readily be explained in terms of just negligibly distorted, trigonal planar $Cu(CN)_3$ units. The situation turns out to be similar for **2**, except that its second Raman active band at 2173 cm^{-1} [6] should now be ascribed to some impurity. Additional work is in progress to clarify if any gold containing congeners of **2** and/or **3** may also be prepared.

7. Experimental

To avoid CO_2 uptake, all preparative work was carried out under an atmosphere of dry nitrogen. Compound **2** was synthesized as reported earlier [6]. Micocrystalline **2** containing in a few cases also some single crystals large enough to be used for an X-ray study grew from the mother liquors obtained after the spontaneous precipitation of comparatively little bulk material, filtration and deposition of the solution at a temperature of ca. 20°C for several weeks.

For the preparation of **3**, a clear solution of $Me_2ClSn(CH_2)_3SnMe_2Cl$ (0.46 g, 1.12 mmol) [18,20] in 20 ml of H_2O was added dropwise to a likewise clear solution of $(^{n}Bu_4N)CN$ (1.21 g, 4.51 mmol) and CuCN (0.40 g, 4.47 mmol) in 40 ml of H_2O, whereafter a white precipitate appeared almost spontaneously. After filtration, washing (three times with small quantities of cold H_2O) and drying in vacuo, the analytically pure product (**3**) was obtained (1.23 g, 1.91 mmol, yield 86%). Decomposition temperature: 170°C; ν(SnC): 495, 525 cm^{-1} (Raman), 551 cm^{-1} (IR). Elemental analysis for $C_{23.5}H_{45}N_5Cu_2Sn$: Anal. Calc. C, 43.87; H, 7.05; N, 10.88; Cu, 19.75; Sn, 18.45. Found C, 43.85; H, 7.19; N, 10.81; Cu, 20.52; Sn, 18.80%.

Preparation of **5**: A solution of $Me_2SnCl(CH_2)_3SnMe_2Cl$ (0.22 g, 0.54 mmol) in 10 ml of H_2O was added dropwise under stirring to a solution of $K[Au(CN)_2]$ (0.31 g, 1.08 mmol) in 40 ml of H_2O. After filtration, washing with small amounts of water and drying in vacuo, pure **5** was obtained (0.26 g, 0.62 mmol; yield: 57%). Decomposition temperature: 305°C (color change from white to yellow); ν(CN): 2186 (Raman), 2166 cm^{-1} (IR); ν(SnC): 556, 533 cm^{-1}, 508 cm^{-1} (Raman), 554 cm^{-1} (IR). Elemental analysis for $C_{5.5}H_9N_2AuSn$: Anal. Calc. C, 26.30; H, 3.61; N, 11.15. Found C, 25.55; H, 3.56; N, 10.85%.

IR spectra were obtained on a Perkin–Elmer IR 1720 instrument, and Raman spectra on a Ramanov U-1000 spectrometer of Jobin Yvon. X-ray powder diffractograms (XRD's) were taken on a Philips PW 1050 instrument (Cu–K_α source and Ni filter). Powder diffractograms were simulated with CERIUS^2 3.0 (MSI) for the 2Θ range 5–70°. The ^{13}C, ^{119}Sn and ^{15}N solid-state NMR spectra were recorded using Varian VXR 300 and Unity Plus 300 spectrometers. Technical details correspond to those given in Refs. [6,18]. Chemical shifts are reported, with the high frequency positive convention, in ppm relative to the signals for $SiMe_4$, $SnMe_4$ and NH_4NO_3 (nitrate line) for ^{13}C, ^{119}Sn and ^{15}N, respectively. Shielding tensor components are defined by $|\sigma_{ZZ} - \sigma_{iso}| \geq |\sigma_{XX} - \sigma_{iso}| \geq |\sigma_{YY} - \sigma_{iso}|$, with anisotropy $\xi = \sigma_{ZZ} - \sigma_{iso}$ and asymmetry $\eta = (\sigma_{YY} - \sigma_{XX})/\xi$.

The crystal structure determination of **2** was performed using an axs Smart-CCD diffractometer. Adsorption corrections based on symmetry equivalent reflections using the SADABS program were accounted for instantaneously by the Smart-CCD diffractometer. The structure of **2** was solved by the direct methods and refined by a full-matrix least-square procedure against F^2 with SHELXS 97 and SHELXL 97.

8. Supplementary data

Crystallographic data for the structural analysis have been deposited with the Cambridge Crystallographic Data Center, CCDC No. 150095 for compound **2**. Copies of this information may be obtained free of charge from The Director, CCDC, 12 Union Road, Cambridge CB2 1EC, UK (Fax: +44-1223-336033; e-mail: deposit@ccdc.cam.ac.uk or www: http://www.ccdc.cam.ac.uk).

9. Note added in proof

Most recently, the new compound $[^nBu_4NCu_3(CN)_4]MeCN$ has been shown to be almost isostructural with **2**, in that each MeSn fragment of **2** is replaced by a two-coordinate Cu(I) spacer [21].

Acknowledgements

This work was supported by the Deutsche Forschungsgemeinschaft (Joint Project: Nano-porous crystals). The CP MAS NMR work was supported by the UK EPSRC (through the National Solid-State Magnetic Resonance Service based at Durham). We also thank Dr F. Olbrich (Otto-von-Guericke-Universität Magdeburg) for collecting the X-ray data set and Mrs S. Samba for her involvement in the successful preparation of single crystals of **2**.

References

[1] E. Siebel, R.D. Fischer, Chem. Eur. J. 3 (1997) 1987.
[2] U. Behrens, A.K. Brimah, T.M. Soliman, R.D. Fischer, D.C. Apperley, N.A. Davies, R.K. Harris, Organometallics 11 (1992) 1718.
[3] K.R. Dunbar, R.A. Heintz, Progr. Inorg. Chem. 45 (1997) 283.
[4] T. Iwamoto, in: D.D. MacNicol, F. Toda, R. Bishop (Eds.), Comprehensive Supramolecular Chemistry, vol. 6, Pergamon, Oxford, 1996, p. 643 and further references given therein.
[5] (a) R.J. Williams, A.C. Larson, D.T. Cromer, Acta Crystallogr. B28 (1972) 858. (b) M.B. Inoue, L. Machi, M. Inoue, Q. Fernando, Inorg. Chim. Acta 192 (1992) 123. (c) M.B. Inoue, M. Inoue, L. Machi, F. Brown, Q. Fernando, Inorg. Chim. Acta 230 (1995) 145.
[6] A.K. Brimah, E. Siebel, R.D. Fischer, N.A. Davies, D.C. Apperley, R.K. Harris, J. Organomet. Chem. 475 (1994) 85.
[7] A.M.A. Ibrahim, J. Organomet. Chem. 556 (1998) 1.
[8] E. Siebel, P. Schwarz, R.D. Fischer, Solid State Ionics 101/3 (1997) 285.
[9] D.T. Cromer, A.C. Larson, Acta Crystallogr. 15 (1962) 397.
[10] (a) U. Greiser, H.H. Wang, K.D. Carlson, J.M. Williams, H.A. Charlier Jr., J.E. Heindl, G.A. Yaconi, B.J. Love, M.W. Lathrop, J.E. Schirber, D.L. Overmyer, J. Ren, M.-H. Whangbo, Inorg. Chem. 30 (1991) 2586. (b) F.B. Stocker, T.B. Staera, C.M. Rienstra, D. Britton, Inorg. Chem. 38 (1999) 984.
[11] A.M.A. Ibrahim, E. Siebel, R.D. Fischer, Inorg. Chem. 37 (1998) 3521.
[12] See: (a) E. Siebel, A.M.A. Ibrahim, R.D. Fischer, Inorg. Chem. 38 (1999) 2530. (b) E.-M. Poll, S. Samba, R.D. Fischer, F. Olbrich, N.A. Davies, P. Avalle, D.C. Apperley, R.K. Harris, J. Solid State Chem. 152 (2000) 286.
[13] See: (a) D. Dakternieks, K. Jurkschat, D. Schollmeyer, H. Wu, Organometallics 13 (1994) 4121. (b) M. Mehring, K. Jurkschat, M. Schürmann, H. Reuter, D. Dakternieks, Angew. Chem. 109 (1997) 1150; Angew. Chem. Int. Ed. Engl. 36 (1997) 1112. (c) M. Mehring, K. Jurkschat, M. Schürmann, I. Paulus, D. Horn, A. Orita, J. Otera, D. Dakternieks, A. Duthie, J. Organomet. Chem. 574 (1999) 176.
[14] (a) P. Schwarz, S. Eller, E. Siebel, T.M. Soliman, R.D. Fischer, D.C. Apperley, N.A. Davies, R.K. Harris, Angew. Chem. 108 (1996) 1611; Angew. Chem. Int. Ed. Engl. 35 (1996) 1525. (b) T. Ogura, E. Shemesh, N. Scott, G.J. Pyrka, Q. Fernando, Inorg. Chim. Acta 149 (1988) 57.
[15] E.-M. Poll, R.D. Fischer, unpublished results.
[16] T. Niu, A.J. Jacobson, Inorg. Chem. 38 (1999) 5346.
[17] R.K. Harris, M.M. Sünnetçioglu, R.D. Fischer, Spectrochim. Acta Part A 50 (1994) 2069.
[18] J.-U. Schütze, R. Eckhardt, R.D. Fischer, D.C. Apperley, N.A. Davies, R.K. Harris, J. Organomet. Chem. 534 (1997) 187.
[19] D.C. Apperley, N.A. Davies, R.K. Harris, A.K. Brimah, S. Eller, R.D. Fischer, Organometallics 9 (1990) 2672.
[20] T.J. Carol, J.P. Hutchinson, J.R. Hyde, H.G. Kuivila, J.A. Zubieta, Organometallics 2 (1983) 106.
[21] G.A. Bowmaker, H. Hartl, V. Urban, Inorg. Chem. 39 (2000) 4548.